Nuclear magnetic resonance evidence of disorder and motion in yttrium trideuteride

John J. Balbach

National Institutes of Health, National Institute of Diabetes and Digestive and Kidney Diseases, Bethesda, Maryland 20892

Mark S. Conradi

Department of Physics, CB 1105, Washington University, St. Louis, Missouri 63130

Markus M. Hoffmann

Pacific Northwest National Lab, Battelle Boulevard, P.O. Box 999, MS P8-19, Richland, Washington 99352

Terrence J. Udovic

NIST Center for Neutron Research, National Institute of Standards and Technology, Gaithersburg, Maryland 20899

Natalie L. Adolphi

Department of Physics, Knox College, Galesburg, Illinois 61401

(Received 10 June 1998)

Three samples of YD_x, with x ranging from 2.9 to nearly 3.0, were studied with deuterium nuclear magnetic resonance to gain insight into the locations of the D atoms in the lattice and their motions. Line shapes at low temperatures (200–330 K) show substantial disorder at some of the deuterium sites. Near 355 K, the spectrum sharpens to yield three uniaxial Pake patterns, reflecting a motional averaging process. However, the three measured intensities do not match the ratios expected from the neutron-determined, HoD_3-like structure. This is strong evidence that the structure and space group of YD_3 are different than reported, or that the current model needs adjustment. At still higher temperatures near 400 K, the Pake doublet features broaden, and a single sharp resonance develops, signalling a diffusive motion that carries all D atoms over all sites. The temperature at which line shape changes occur depends on the number of deuterium vacancies, $3-x$. The changes occur at lower temperatures in the most defective sample, indicating the role of D-atom vacancies in the motional processes. The longitudinal relaxation rate T_1^{-1} displays two regimes, being nearly temperature independent below 300 K and strongly thermally activated above. The relaxation rate depends on the number of deuterium vacancies, $3-x$, varying an order of magnitude over the range of stoichiometries studied and suggesting that D-atom diffusion is involved. Also, the activation energy describing T_1^{-1} ($\simeq k_B \times 5500$ K) approximately matches that for diffusion. An unusual $\omega_0^{-0.7}$ frequency dependence of T_1^{-1} is observed. A relaxation mechanism is proposed in which diffusion is the rate-determining step and in which frequency dependence arises from a field-dependent radius of the relaxation zones. [S0163-1829(98)07845-X]

I. INTRODUCTION

Recently, Huiberts and co-workers prepared a thin layer of metal hydride with remarkable properties.[1–4] By controlling the hydrogen content between 2 and 3 stoichiometric units, a reversible metal-insulator transition could be induced, resulting in a switchable mirror. This finding has generated increasing interest in the yttrium hydride system. Evidently, the thinness of the yttrium film plays a crucial role since bulk dihydride decrepitates (falls apart into powder) due to the strains encountered during the transition to the trihydride phase. Whether surface effects in these thin films play a crucial role in the observed metal-insulator transition is yet to be determined.

There has been some controversy surrounding the theoretical treatment of this system. Early band-structure calculations[5] predicted that YH_3 has a band gap, in agreement with the measurements on the films. However more recent theoretical work on YH_3 (Refs. 6–8) finds band overlap, assuming the YH_3 is in the HoD_3-like structure, as determined by recent neutron powder diffraction[9] on YD_3.

Displacements of the H(D) from the HoD_3 structure have been calculated to lower the total energy and to yield a small band gap.[10,11] Electron correlation effects (beyond the local-density approximation) have been suggested to result in a band gap in YH_3.[12] And one group has found a band gap for YH_3 in the undistorted structure, without invoking strong electronic correlations.[13] Thus, while the experimental result of a ≈ 1.8-eV gap in the film is certain, the theoretical explanation of the facts is as yet unclear.

The basic model of structure for YD_3 used to fit the neutron powder diffraction[9] data is the same structure found for HoD_3,[14] with space group $P\bar{3}c1$. This is a distortion of a simple hcp structure, with the unit cell larger in the a-b plane by $\sqrt{3} \times \sqrt{3}$. There are three different types of interstitial sites for H(D) atoms; their origins may be understood as the 12 tetrahedral and six octahedral sites (per six metal atoms) of the undistorted hcp structure. In the enlarged unit cell of six metal atoms, there remain 12 distorted tetrahedral sites, all crystallographically equivalent. The six octahedral sites become four sites slightly above and below the metal-atom planes and two sites in the plane. Thus the numbers of sites

are in the ratio 12:4:2 (tetrahedral:near plane:in plane), in the HoD_3 structure.

The model was expanded from the HoD_3 structure to introduce *disorder* in the D-atom system of YD_3. In Ref. 9 the disorder is described by model V, the best fitting of the several structural models. The data were interpreted as a fraction f of near-plane D atoms moving to in-plane sites. The nearby in-plane D atoms move to near-plane sites that are similar but not identical to the abandoned near-plane sites. The extent of the disorder gently increases with temperature, the fraction f growing from 0.13 at and below 200 K to 0.18 at 400 K. The temperature independence of f below 200 K is believed to indicate kinetically frozen-in disorder. All of the models used to fit the neutron data had relatively large thermal factors for each site, except for the near-plane and in-plane sites when disorder was explicitly included.

Earlier electric-field-gradient (EFG) determinations[15] from perturbed angular correlation measurements of the yttrium sites substituted by Ta atoms also found evidence of significant disorder. In addition, a change in the EFG between 300 and 400 K was interpreted as a phase transition to a higher-symmetry, more ordered structure. This phase transition (different from the dihydride-trihydride transition) was not seen by the neutron-diffraction experiments.

Deuterium nuclear magnetic resonance (NMR) is sensitive to the EFGs at the D-atom sites through the quadrupole interaction. Because the EFG is a probe of the local symmetry, deuterium NMR should provide insight into the local structure, complementary to the neutron-diffraction data. In the HoD_3-like structure, two of the three different deuterium sites [the in-plane $D(m1)$ and near-plane $D(m2)$ sites] should have uniaxially symmetric EFGs, with the c axis being the unique axis.[9] These D-atom sites have only three nearest metal-atom neighbors and should have correspondingly strong EFGs. The so-called tetrahedral sites have lower than threefold symmetry (there are three different distances to the four nearest Y atoms in the HoD_3-like structure) and are not expected to have a uniaxially symmetric EFG. On the basis of the *approximate* tetrahedral symmetry of these sites, one expects weak EFGs. Thus, for the HoD_3-like structure, we expect the powder spectrum to be the superposition of two uniaxial Pake powder doublets and a narrower pattern corresponding to the tetrahedral sites. The intensities of these components should be in the same ratios as the numbers of sites—6 tetrahedral $D(t)$ sites: 2 near-plane $D(m2)$ sites: 1 in-plane $D(m1)$ site.

The Pake doublet line shape[16] occurs because, in powder samples such as here, all orientations of the EFG with respect to the magnetic field are equally represented. Although Pake doublets *can* arise from dipole-dipole interactions, these interactions are too weak with deuterons to explain the observed Pake splittings (linewidths). Because the strength of the EFG directly determines the Pake splittings and because each distinct D-atom site has an unique EFG, different Pake splittings arise from the distinct D-atom sites.

Atomic motions such as diffusion are clearly important in the optical switching behavior of the yttrium film,[2] allowing for bulk D-atom transport. Motion of the D atoms will modulate the EFG seen by an individual deuterium spin and will be detectable by its effects on the line shape and on relaxation rates.

Frequency shifts (primarily Knight shifts[16]) provided much insight into the behavior of $YD_{2+\Delta}$.[17] However, as YD_3 is nonmetallic, we expect no detectable shifts in this system. Indeed, magic-angle spinning spectra of YD_3 show only a single, featureless line.[18]

Weaver examined proton NMR in samples of YH_x, with x ranging from 2.61 to 2.94.[19] Surprisingly, at low x where two phases (nominally dihydride and trihydride) coexist, single-component NMR signals were observed. At large x where a single phase was expected, two-component NMR signals were found. Much has been learned about the necessity of careful YH_x sample preparation[20] since the early work.

II. EXPERIMENT

The first sample examined by deuterium NMR was received from NIST and was powder from the same batch as the samples used in the neutron-powder-diffraction measurements. The sample preparation is described elsewhere;[9] the sample may have *slightly* less D content than in Ref. 9 due to brief sample handling in a non-D_2 atmosphere. The sample was sealed in Pyrex under an argon atmosphere. The Y metal (metals purity 99.99%) had been obtained from Johnson Matthey Co. The NIST sample was described as having a D/Y ratio of 3 (no error limit); we believe the D/Y ratio is quite near (but slightly less than) that of the $YD_{3.0}$ sample (see below).

After the initial measurements, we became concerned that very small amounts of paramagnetic impurities might have an effect on the longitudinal relaxation rates.[21] To investigate this, additional samples were prepared with Y metal (metals purity 99.999%) received from the Materials Preparation Center at Ames Laboratory, Ames, IA. The Ames metal was deuterided at Washington University in a manner similar to the NIST sample. Each of the two samples began as several metal chunks of about 2 g each. After annealing at 900 K for 12 h under carefully trapped vacuum, D_2 gas was slowly admitted to the sample vessel to limit the temperature increase from the exothermic uptake reaction. To accommodate the much higher vapor pressure of YD_3, when the metal reached the dideuteride concentration (as indicated volumetrically), it was allowed to cool slowly under 700 Torr of D_2 gas to near 550 K. As gas was absorbed, it was replaced to keep the pressure relatively constant. When the sample no longer absorbed deuterium, it was cooled to room temperature under D_2 gas, and the total amount of gas absorbed was calculated volumetrically. The deuterided samples were powder with a shiny black appearance. The slow cooling approach is common in synthesizing YD_3; the idea is that the sample will spend a sufficiently long time at a temperature where both the kinetics (absorption rate) and thermodynamics (D_2 vapor pressure) permit a nearly complete uptake of the D atoms.[9,20] The technique was successful — the first sample was calculated to be $YD_{3.02}$. As discussed below, given the measurement uncertainties, we call this sample $YD_{3.0}$. The second sample was reheated to 300 °C after being fully loaded, to drive off some of the absorbed deuterium. The amount of gas driven off was measured, and a new, lower stoichiometry was achieved: $YD_{2.9}$. The sample was allowed to homogenize for 4 h at 300 °C. This sample

proved to be valuable in demonstrating the role played by D-atom vacancies.

The amount of absorbed deuterium was calculated volumetrically. First, a standard volume was measured by weight when filled with water, carefully degassed to remove bubbles. The volumes of the other regions of the apparatus were deduced by determining pressure ratios using a linear pressure transducer (Edwards Datametrics Barocel) as a fixed quantity of gas was allowed to expand into successive volumes. The volumes were determined to an accuracy of 1%. The mass of each set of metal pieces was determined to within 0.1%; thus the uncertainty in the volumetric measurements determined the inaccuracy in metal-deuteride stoichiometry. The two samples had measured deuterium-to-metal ratios of 3.02 ± 0.03 and 2.90 ± 0.03. The samples are referred to as $YD_{3.0}$ and $YD_{2.9}$, respectively. During preparation, the samples were stored under dry N_2 gas, to avoid oxidation. After deuteriding, the samples were sealed into Pyrex vessels under 0.7 bar of D_2 gas. The use of sealed samples prevented the evolution of deuterium gas at high temperatures. Indeed, no changes in the samples' NMR behaviors were noted throughout the several months of study. Detailed protocols of the sample preparations can be found in Appendix C of Ref. 22.

Most of the NMR measurements were carried out in an 8.4-T superconducting solenoid with an 89-mm bore diameter. Some lower field work at 1.0 and 2.0 T was performed in an iron-core electromagnet with NMR field stabilization. Early measurements of the deuterium spectrum were done on a homemade NMR spectrometer. The bulk of the measurements, including all of the T_1 and T_2 measurements, were made with a Chemagnetics CMX-360 spectrometer. All spectra were obtained by Fourier transformation of the spin echo from a 90_x-τ-90_y pulse sequence, with phase alternation $(x,\bar{x})$ of the first pulse for artifact cancellation. The pulse widths were 4 μs. The probes were temperature controlled by flowing nitrogen gas. Temperatures were measured with a type-T thermocouple mounted next to the sample vessel. Temperature control was typically to $\pm 0.5\,°C$; reported temperatures are believed to be accurate to $\pm 2\,°C$, with relative temperatures more precise ($\pm 1\,°C$).

III. RESULTS AND DISCUSSION

A. Low-temperature spectrum

Spectra of all three samples are presented in Fig. 1 at several temperatures. The spectra obtained at the lowest temperature, 200 K, are particularly important because they should be unaffected by atomic motions such as diffusion. Indeed, the spectra of $YD_{3.0}$ and the NIST sample change very little up through 330 K. Thus, these spectra reflect the static distribution of electric field gradients (EFGs) in the material.

The spectra at 200 K of $YD_{3.0}$ and the NIST sample are quite similar. The features at ± 14 kHz are cusps (singularities) of a uniaxial Pake powder doublet;[23] in some of the spectra the corresponding steps at ± 28 kHz are visible. The cusps of the NIST sample are less pronounced than in the $YD_{3.0}$, reflecting some broadening in the NIST sample.

The spectrum of $YD_{2.9}$ at 200 K is very similar to that of $YD_{3.0}$, with the exception of the 3-kHz-wide line centered at
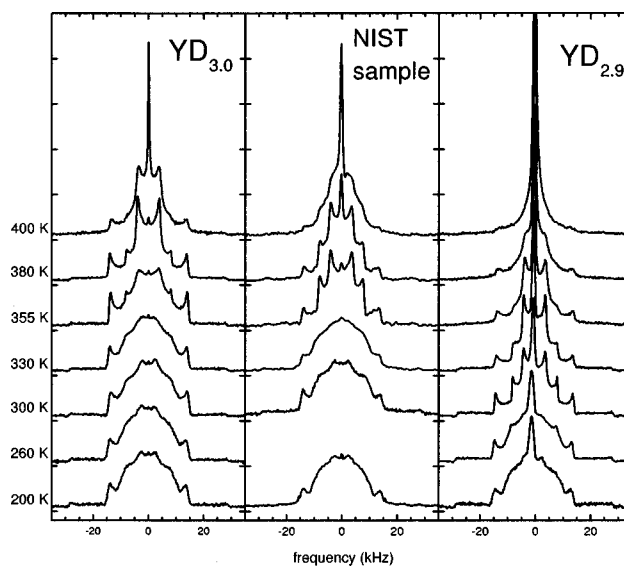

FIG. 1. Deuterium NMR spectra of three samples of nominal YD_3. The spectra are presented, left to right, in order of descending D-atom content. For all three samples, the resonance spectra show disorder and/or nonuniaxially symmetric EFGs at low temperatures. At higher temperatures, a superposition of three Pake powder doublets is evident. At the highest temperatures, the Pake doublet features broaden, and a single sharp line appears. The temperatures at which spectral changes appear are lowest for $YD_{2.9}$.

-1.5 kHz in $YD_{2.9}$. This feature is the resonance line of the cubic metallic $YD_{2+\Delta}$ dideuteride phase, as shown by the agreement with the known linewidth, shorter T_1, and Knight shift of $YD_{2+\Delta}$.[17,24] The appearance here of the dideuteride resonance is due to the concentration gap (two-phase coexistence region) between the dideuteride and trideuteride phases. Evidently, the low concentration limit of the trideuteride phase is greater than $x=2.9$, much higher than the previously published value of 2.7 for this system.[25–27] Indeed, neutron powder diffraction readily detects the presence of $YD_{2+\Delta}$ ($\Delta \simeq 0.08$) after intentional removal of deuterium from nominally YD_3, revealing the phase boundary at room temperature to be well above $x=2.9$.[28]

The excellent agreement between the spectra of all three samples at 200 K (after subtraction of the $YD_{2+\Delta}$ feature from the $YD_{2.9}$ spectrum) indicates that the distribution of EFGs is the same for all three. Thus, the EFGs do not arise primarily from deuterium vacancies (of concentration $3-x$) but are intrinsic to the trideuteride structure.

According to the discussion in the Introduction, the expected spectrum of the HoD_3-like structure is a superposition of two uniaxial Pake doublets from near-plane and in-plane sites and a narrower, not necessarily uniaxial component from tetrahedral sites. The intensity ratios are expected to be 2:1:6, respectively. The only way to map the observed low-temperature spectra onto the expected spectrum is to associate the 28-kHz doublet (all doublets will be referred to by their cusp-to-cusp frequency width) with *both* the near-plane and in-plane D atoms. The rather featureless central part of the spectra in Fig. 1 then arises from the tetrahedral D atoms, $D(t)$. Although it is difficult to separate broadened resonance lines, we find the 28-kHz doublet accounts for 30–40% of the total intensity, in agreement with the expected 33%.

This spectral assignment invokes equal EFGs for the near-plane and in-plane sites, either by chance or because of their similar local structures. Indeed, the Y-D nearest-neighbor distances in Ref. 9 are quite similar: 2.15 and 2.13 Å (see p. 431, model V, 295 K of Ref. 9). Motional averaging can be ruled out here because of the absence of any temperature dependence from 200 K to 330 K (YD$_{3.0}$ and NIST samples) in Fig. 1. The central, featureless resonance assigned to tetrahedral D atoms cannot be modeled with a single EFG, whether of uniaxial symmetry or not. Instead, it appears that these sites are in a substantially disordered environment. That is, the D(t) atoms sit in a distribution of local environments. This may explain the large thermal factors found for the D(t) sites in model V of the neutron study.

Spectra were obtained at a lower field, corresponding to 13.05 MHz, in the YD$_{3.0}$ sample and at 293 K. The lower field spectra (not shown) are of lower S/N but otherwise unchanged, compared to 8.4 T and 54.36 MHz. Thus, magnetic susceptibility broadening in our powdered samples is negligible.

B. Spectral changes with temperature

With increasing temperature, the spectrum of each sample in Fig. 1 evolves into a superposition of three Pake powder doublets of uniaxial symmetry. For YD$_{3.0}$ and the NIST sample, this is most evident at 355 and 380 K; for YD$_{2.9}$ three sharp doublets are already clear at 300 K. The simplest explanation for the sharpening is a motion of D atoms that averages away the disorder present at 200 K. It is important to note that the outer, 28-kHz Pake doublet shows little broadening at low temperature and is hardly affected by the sharpening process. Thus the sharpening involves primarily the resonance of the tetrahedral sites, according to our spectral assignment. The D-atom vacancies are certainly important in the motional averaging, as demonstrated by the more defective YD$_{2.9}$ sample that has more D-atom vacancies. The spectral features of the YD$_{2.9}$ sample sharpen at a much lower temperature than the spectral features of the other two samples. However, the averaging motion that leads to the spectral sharpening cannot involve an appreciable rate of D-atom *interchanges* between the different sites. Such interchanges would create a single resonance, because all D atoms would be equivalent on time average. Instead, the spectral sharpening must involve small displacements of the atoms or hopping betweeen nearby subsites (subsites are too close to allow simultaneous occupation).

The relative intensities of the three Pake powder patterns must be determined with care. First, all three doublets should be equally longitudinally relaxed; we accomplished this by allowing full relaxation to occur, using a delay interval of several times T_1. As shown below, all three resonances display the same T_1 so this is not a major issue. Second, the three lines have different transverse relaxation times T_2. We measured the relative intensities from spin echoes (90$_x$-τ-90$_y$-τ-echo pulse sequence) and extrapolated to the $\tau=0$ limit. The relative intensities at $\tau=20$ μs (the shortest τ employed) were no more than 25% different than the extrapolated values; typically, the difference was only 10%.

We used smooth curves to separate the observed spectra into three components; alternatively we used a mathematical deconvolution based on the three ideal Pake patterns (three cusp-to-cusp splittings of 28, 16, and 9 kHz). The ideal spectra were treated as vectors and orthogonalized to produce an orthonormal basis for decomposition of the observed spectra. The relative intensities were (28 kHz doublet: 16 kHz doublet: 9 kHz doublet) 41:21:38 for the YD$_{3.0}$ sample at 379 K, 45:25:30 for the NIST sample at 352 K, and 36:29:35 for the YD$_{2.9}$ sample at 298 K. The values obtained with the two methods agreed reasonably, so that each value is uncertain to $\pm 5\%$ (e.g., $40\pm5:30\pm5:30\pm5$). All of the ratios measured are far from the result expected for a HoD$_3$-like structure of 67:22:11. Thus, the three doublets cannot be directly attributed to the three kinds of D-atom sites.

The motional averaging responsible for the sharpening of the doublets is fairly modest in amplitude. The overall computed second moments do not vary much from 200 to 380 K. At the frequencies of the cusps of the intermediate and innermost doublets, there are residual features present in the low-temperature spectra. All of this indicates that the EFGs arising from the (assumed) disorder at low temperature are somewhat smaller than the EFGs remaining after motional averaging.

Importantly, the temperature region in which the deuterium Pake patterns sharpen and become most evident is also the region in which measurements of the EFG at the yttrium site[15] gave evidence of a phase transition from a disordered structure to a more symmetric one. We suggest that the yttrium-site EFG data do *not* indicate a phase transition, but a gradual change with temperature due to motional averaging, just as for the present deuterium spectra.

At still higher temperatures, the Pake features broaden and a sharp central line begins to grow. For the least defective samples, the YD$_{3.0}$ and the NIST sample, this is apparent at 400 K. For YD$_{2.9}$, this process begins at approximately 355 K. Hence, just as with the sharpening process that resulted in the superposition of three Pake powder doublets, the vacancy concentration $3-x$ is important; a higher vacancy concentration yields the same averaging effect at a lower temperature (for example, compare YD$_{3.0}$ at 400 K and YD$_{2.9}$ at 355 K). Based on these effects, we believe the NIST sample has a D/Y ratio only slightly less than the YD$_{3.0}$ sample and substantially more than the YD$_{2.9}$ sample.

The collapse to a single line indicates that vacancy diffusion is occurring, resulting in diffusion of the D atoms between the many sites. The averaging over the sites causes a broadening of the three Pake powder patterns that can be understood as lifetime broadening ($\Delta f \Delta t \sim 1$). Also, an averaged central resonance line appears. That the sharpened line begins to emerge before the Pake doublets have been completely broadened reflects the powder sample (some crystallite orientations will average at lower temperature than others) and, evidently, a distribution of hopping rates. We note that the crystal structure is a variation on hcp, so there is no reason based upon symmetry that the average EFG over all sites should be zero. But it *is* zero, as indicated by the lack of any splitting in the averaged spectrum (i.e., in the narrow spike at 400 K).

The observed onset of motional narrowing allows us to determine an activation energy for the diffusive motion. Since the averaging requires motion on the 10^{-5} s time

scale (the reciprocal of the mean linewidth in radians per second), we can determine the activation energy by

$$\tau_e = 3 \times 10^{-12} \exp\left\{\frac{E_a}{k_B T}\right\} \quad \text{s} \tag{1}$$

and by setting the exchange time $\tau_e = 10^{-5}$ s at 400 K, as appropriate for YD$_{3.0}$. The prefactor was chosen as the reciprocal of the product of a typical D-atom vibration frequency and the vacancy concentration ($\approx 10^{-2}$). The activation energy calculated in this manner is $E_a/k_B = 6000$ K, with large error limits (6000 ± 1000 K).

There is evidence that the diffusing vacancies are concentrated most heavily on the subset of D-atom sites giving rise to the intermediate-width (16-kHz) Pake doublet. In Fig. 1, the spectrum of YD$_{2.9}$ changes from 300 K to 330 K to 355 K mostly by diminishing the cusp of the intermediate-width Pake pattern; the outermost and innermost doublets are affected only at higher temperatures. A similar situation is evident in Fig. 1 for YD$_{3.0}$ at 400 K (compare to YD$_{2.9}$ at 355 K). We note that diffusion of vacancies on a subset of sites will cause the D atoms to interchange among the subset of sites. Even though the sites are energetically equivalent (and hence have the same EFG principal values), the EFG tensors on the sites generally have different *orientations*. Thus vacancy diffusion on a subset of sites will cause motional broadening of the resonance from these sites (exceptions to this reasoning include the near-plane and in-plane sites, where the EFG tensors all have the same orientation, with the unique axis along c).

At one time we considered the possibility that the central line is from D$_2$ gas desorbed from the sample. However, to account for the most intense central line observed (in YD$_{2.9}$ at the highest temperature) would require a D$_2$ pressure over 100 atm, which would surely rupture the glass vessel. Furthermore, the central line is most intense for a given temperature in YD$_{2.9}$ (see Fig. 1), while the vapor pressure is known to rise rapidly as the last sites are filled ($x \rightarrow 3$). Additionally, the samples were prepared with D$_2$ pressures $\lesssim 1$ bar at higher temperatures than 400 K, so the vapor pressure at 400 K will be much less than 1 bar. Finally, we observe a single T_1 for the sharp line and the broadened remnants of the Pake patterns. The gas and solid would be expected to have different T_1's unless in rapid exchange. Thus, the sharp central line is definitely not from desorbed D$_2$ gas.

The main features of the deuterium spectra are summarized now. (1) The low-temperature spectra reveal disorder. The low-temperature spectra are the same for all three samples, showing that the amount of disorder does not depend on the vacancy concentration. The 28-kHz doublet is assigned to near-plane and in-plane D atoms, with the featureless (disordered) central region due to tetrahedral D atoms. The spectra reflect quadrupolar interaction with EFGs, since the line shapes are independent of field. (2) Upon heating to 355–380 K, the central region of the spectrum develops into two uniaxial Pake doublets, 16 and 9 kHz wide. Their intensities are approximately in the ratio 3:4, respectively; we cannot ascertain whether the ratio is sample dependent. (3) Further heating to 400 K leads to broadening of the Pake features and growth of an averaged, central line;

these changes are due to vacancy diffusion, allowing the D atoms to interchange among the sites. The activation energy calculated for this diffusion is 6000 K$\times k_B$. (4) Items 2 and 3 occur at markedly lower temperatures in the sample with the most D-atom vacancies, demonstrating that vacancy-mediated diffusion is important for both motion processes.

The most difficult features of the line-shape data to explain are the nature of the disorder, the motion that averages the disorder, and the division of the signal of the tetrahedral D atoms into two distinct doublets (16 and 9 kHz). The neutron-powder-diffraction data also indicate the presence of disorder but primarily involving vertical (c-axis) displacements of the near-plane and in-plane D atoms. In turn, these displacements may affect the EFGs of the tetrahedral D atoms. The neutron data also indicate some disorder in the locations of the tetrahedral D atoms.

We do not know the nature of the disorder and the motion that averages it. Nevertheless, this much is firmly based on the deuterium NMR data: The local structure is markedly different than the averaged (or long-range) structure from the neutron data. In particular, the six tetrahedral D(t) atoms are most affected by the distortion away from the average structure. The distortion may make inequivalent the D(t) atoms in one unit cell, or from one cell to the next, or both. The distortion is not due directly to D-atom vacancies, but motion of the vacancies is involved in the averaging of the distortion. After averaging, the D(t) atoms find themselves in two distinct groups of roughly equal numbers with different (time-averaged) EFGs. Thus, even after the motional averaging of the distortion, the D(t) atoms have not regained their equivalence (as in the neutron-determined, long-range HoD$_3$ structure).

Recently, it has been reported[29] that the neutron-diffraction results can also be fit with space group $P6_3cm$. This structure has the six D(t) atoms divided into two groups of three equivalent atoms each. It is unclear as yet whether this structure is in accord with the neutron vibration spectrum, however. Still, in this structure, the nearly 1:1:1 intensity ratio of the deuterium Pake patterns is the expected result. Thus, the NMR spectra indicate that $P6_3cm$ may well be the correct space group. There may also be modifications to the $P\bar{3}c1$ space group that would split the tetrahedral sites into two groups. These modifications include disorder of the T sites (which has not been explicitly introduced to the neutron-data models), twinning (where there are two structures that are mirror images), and short-range distortions of the structure that escape detection by neutron diffraction.

We offer the following speculation concerning the disorder and its motional averaging. The shift of the in-plane and near-plane D atoms [D(m1) and D(m2) in Ref. 9] form a wave in the a-b plane. Indeed, a major difference between space groups $P\bar{3}c1$ (the HoD$_3$-like structure) and $P6_3cm$ is the phase of this distortion wave, relative to the underlying periodic lattice. If the distortion wave were incommensurate with the lattice, it might be pinned at low temperatures and mobile at high temperatures. Indeed, a distortion wave might be pinned to one or more D-atom vacancies, so that vacancy motion would control the motion of the distortion wave. Assuming that displacements of the in-plane and near-plane D atoms generate changes in the EFGs of the D(t) atoms, this could explain the disorder at low temperature and spectral
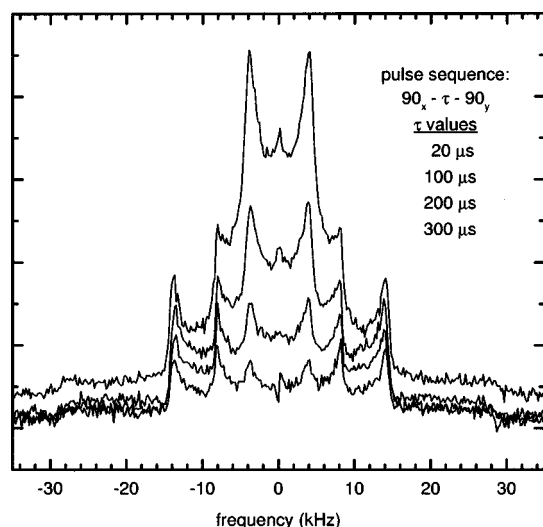
FIG. 2. Spectra from two-pulse spin echoes with various delay times τ(20 μs is plotted on top). All data are from the NIST sample at 352 K. The cusps of the outermost doublet (at ± 14 kHz) are attenuated least by the increasing τ values. The innermost doublet (cusps at ± 4.5 kHz) is attenuated most rapidly. The differences in the apparent T_2^{-1} show the extent to which the inequivalent D-atoms's quadrupole interactions are differently modulated by atomic motions.

sharpening evident in Fig. 1. We note that no diffraction evidence of incommensurate distortions has appeared; short-range distortions would be difficult to detect, however.

C. T_2 and spin-alignment echo data

In all spin-echo experiments, the echo will have a maximum amplitude if a typical spin's frequency during the dephasing interval equals its frequency during the rephasing interval. Thus, spins with stochastically varying frequencies will yield echoes with an increased decay rate T_2^{-1}.

In the temperature regions where the deuterium NMR spectra showed multiple components (i.e., the three doublets and the central spike), the components generally displayed different transverse relaxation rates T_2^{-1}. Figure 2 presents spectra from the NIST sample at 352 K; with increasing pulse delay interval τ, the cusps of the innermost doublet decrease more rapidly than the other features. Clearly, the quadrupole interactions of the spins producing the innermost doublet are fluctuating stochastically at this temperature.

Figure 3 reports T_2 measurements for the NIST sample, where the decay of the total echo amplitude is reported. That is, no attempt has been made to separate the several spectral components. Below 300 K the T_2 (the value of 2τ for decay by $1/e$) is temperature independent and the echo decay envelope is Gaussian, indicating that the decay is due to deuterium like-spin dipolar interactions (not atomic motion). Indeed, the 500-μs T_2 is typical of perdeuterated solid organic compounds,[30] systems with densities of deuterium atoms similar to YD$_3$. Above 300 K, the decay envelope becomes more exponential, and T_2 decreases. Both of these findings are in accord with transverse relaxation from fluctuating spin frequencies (most likely, fluctuating quadrupole interactions due to motions).
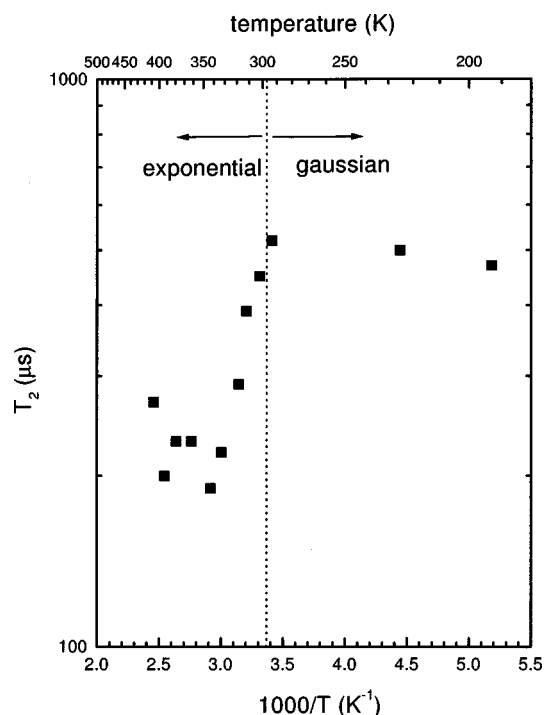

FIG. 3. T_2 measurements on the NIST sample. The measured T_2 represents the decay of the spin-echo envelope and thus is an average over the sites. Above 300 K, T_2 is shorter and describes an exponential decay. This suggests that motion-driven fluctuations in the quadrupole interaction control T_2 above 300 K.

The spin-alignment echo is a three-pulse echo that allows *slow* variations in quadrupole interaction to be detected.[30] Data from the NIST sample are presented in Fig. 4, at temperatures well below the onset of line-shape changes. The echo amplitude is plotted as a function of the delay time between the second and third pulses; the first two pulses are separated by a fixed 100 μs. At 165, 195, and 241 K, the decays are nearly the same, indicating that spectral diffusion through deuterium like-spin dipolar interactions is responsible. But at 265 and 288 K, the decay is much more rapid, due to stochastic variations in the quadrupole interactions. At these temperatures, the spin-lattice relaxation time T_1 is approximately 1000 s and has negligible effect on the decays in Fig. 4. Thus, even at 265 K, the quadrupole interactions are varying because of the D-atom motions, though the variations are on a long time scale.

D. T_1 data

The spin-lattice relaxation rate T_1^{-1} is reported in Fig. 5 for each sample as a function of temperature at 54.36 MHz (8.4 T). Excepting the YD$_{2+\Delta}$ phase in the YD$_{2.9}$ sample, T_1 was uniform across the entire multicomponent spectrum, and the recovery function was a single exponential. In light of the different T_2 values of the several components, this is surprising and can only be explained if the D atoms can exchange over all the D sites in a time much shorter than T_1, resulting in a single relaxation rate. This same exchange process leads at higher temperatures to the broadening of the Pake features and the development of the central spike in the spectrum (see Fig. 1). Motional averaging requires exchange on the 10^{-5} s
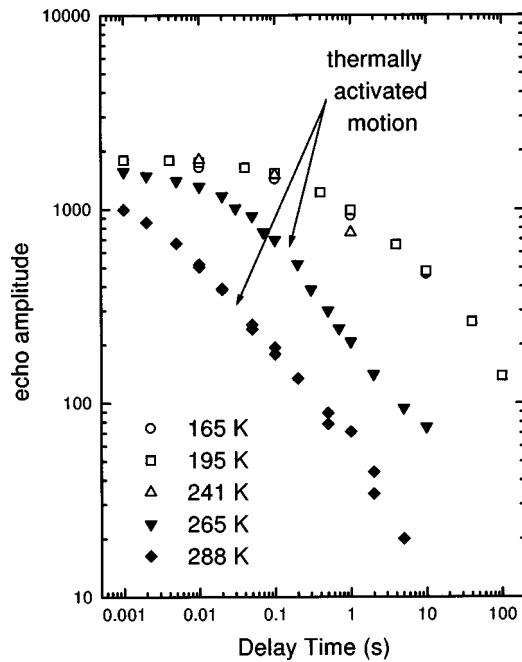
FIG. 4. Decay of spin-alignment echoes for the NIST sample as a function of the second delay interval. At the lowest temperatures, the decay is independent of temperature, suggesting that the slow decay is from rigid-lattice dipolar interaction. At higher temperatures, the echo decays more rapidly and at a temperature-dependent rate. Here, the decay is from fluctuations in the quadrupole interaction, driven by atomic motions.

time scale, while homogenization of the T_1 decay requires only one exchange per time T_1 (as long as 10^3 s at low temperatures). We can determine the exchange time τ_e from Eq. (1) using the activation energy calculated for the diffusive motion. At 200 K, the exchange time is still only 32 s, much shorter than the ≈ 1000-s T_1. Thus the observation of a single T_1 over all sites is *expected* in light of the D-atom diffusion.

At low temperatures, T_1^{-1} becomes nearly independent of temperature. As in Fig. 5, the plateau value of T_1^{-1} does not appear to be directly linked to the concentration of vacancies $3-x$. Thus, it is reasonable to assume that the longitudinal relaxation in this region is from paramagnetic impurities and is spread slowly by spin diffusion. However, T_1^{-1} in the thermally activated region above 300 K is sensitive to the concentration of vacancies, with faster relaxation in the most defective sample. Over the three samples, T_1^{-1} varies by an order of magnitude. We note that the T_1^{-1} of the NIST sample is intermediate between those of YD$_{3.0}$ and YD$_{2.9}$ in the thermally activated region, further evidence that the stoichiometry of the NIST material is intermediate (and closer to YD$_{3.0}$).

Figure 6 shows the frequency dependence of T_1^{-1} found in the NIST sample. The relaxation rate T_1^{-1} varies as $\omega_0^{-0.7}$ in the thermally activated regime, over almost a decade in frequency. To test the possibility that the frequency dependence of T_1^{-1} is influenced by small amounts of inevitable paramagnetic impurities, measurements were performed on the two samples with extremely high-purity metal from Ames Laboratory. Figure 7 shows the field dependence of the high-purity samples. The frequency dependences of the
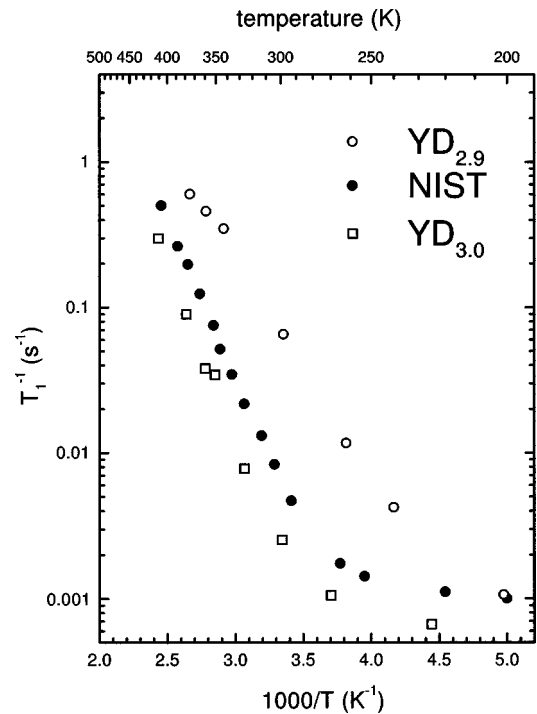

FIG. 5. Relaxation rate T_1^{-1} for all three samples at 8.4 T. There are two temperature regimes, as seen most distinctly for the NIST sample. Below 250 K, T_1^{-1} is more or less independent of temperature. Above 300 K, T_1^{-1} increases according to a thermally activated process. Note that the rates T_1^{-1} increase markedly in the high-temperature region as the sample is made increasingly substoichiometric.

YD$_{3.0}$ and YD$_{2.9}$ samples in the thermally activated regime are approximately $\omega_0^{-0.65}$ and $\omega_0^{-0.6}$, respectively, extremely similar to the NIST sample's behavior. An analysis of the Y metal from Johnson Matthey indicated that the total concentration of paramagnetic impurities like Gd or Ni in the NIST sample is about 40 ppm, only a factor of 2 or 3 greater than in the Ames Laboratory starting material.

The observed T_1^{-1} behavior with temperature and frequency is very unusual, and we consider what mechanisms could be responsible. There are two general relaxation mechanisms available to the D atoms, quadrupolar and magnetic. If the longitudinal relaxation is quadrupolar, we expect the rate to be given at least approximately by simple theory,[16]

$$T_1^{-1} = M_2 J(\omega_0), \quad (2)$$

with a constant (independent of temperature) second moment M_2 describing the fluctuations in the quadrupolar interactions. Here $J(\omega_0)$ is the normalized spectral density at the spin precession angular frequency ω_0 and is often taken to be Lorentzian:

$$J(\omega_0) = \frac{\tau_c}{1 + \omega_0^2 \tau_c^2}, \quad (3)$$

with τ_c being the correlation time of the fluctuations. Thus, to explain the increasing T_1^{-1} with increasing temperature, one must assume that $\omega_0 \tau_c \gg 1$ (since τ_c is assumed to de-
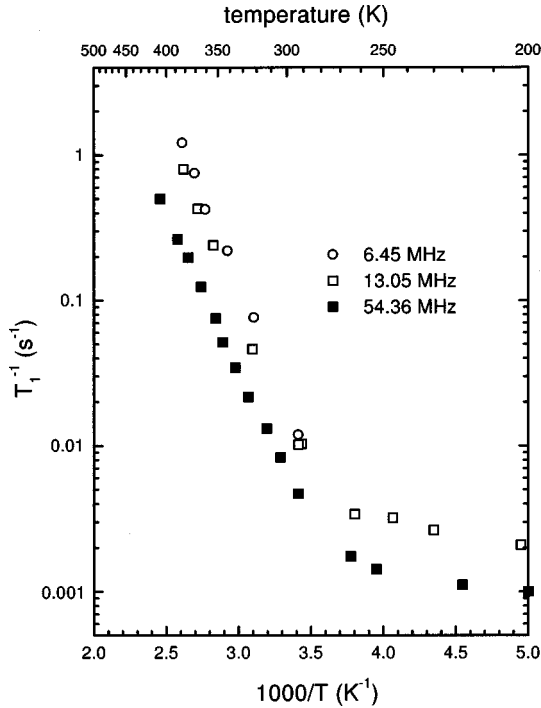
FIG. 6. Relaxation rate T_1^{-1} at three frequencies in the NIST sample. A weak frequency dependence ($\approx \omega^{-0.7}$) is apparent in both temperature regimes. Note the wide range of measurement frequencies.

FIG. 7. Frequency dependences of T_1^{-1} of the $YD_{3.0}$ and $YD_{2.9}$ samples. The frequency dependence is approximately the same as for the NIST sample, as in Fig. 6.

crease with increasing temperature). But in this limit, T_1^{-1} varies as ω_0^{-2}, a much stronger variation than observed. Thus, quadrupolar relaxation cannot explain the observed T_1^{-1}.

We now calculate the quadrupolar relaxation rate T_1^{-1} expected in YD_3 due to the diffusive motion responsible for broadening the Pake features and development of the sharp spike near 400 K. We need to show that the quadrupolar relaxation is smaller than the observed relaxation. Following Abragam,[23] we find in the slow fluctuation limit $\omega_0 \tau_c \gg 1$,

$$T_1^{-1} = \left(\frac{3}{20}\right)\left(1 + \frac{\eta^2}{3}\right)\frac{\overline{(\Delta f)^2}}{f_0^2 \tau_c}, \qquad (4)$$

where f_0 is the resonance frequency (in cycles per second) and the correlation time τ_c is given by the exchange time τ_e. Each Pake pattern has uniaxial symmetry ($\eta = 0$) and cusp-to-cusp splitting Δf. We obtain the mean-squared splitting by assuming the three doublets have equal weights, with splittings of 9, 16, and 28 kHz. At 400 K where τ_e is 10 μs from Eq. (1), T_1^{-1} will be 0.04 s^{-1} at 13.05 MHz and 0.0023 s^{-1} at 54.36 MHz. Thus, quadrupolar spin-lattice relaxation is smaller by at least a factor of 10 than the observed relaxation (Figs. 5 and 6). Presumably, since the quadrupolar relaxation varies as f_0^{-2}, it would dominate only at much lower frequencies.

Thus, we must turn to magnetic sources of relaxation. We start by noting that D-atom diffusion is closely linked to the spin-lattice relaxation in this material. First, the activation energy that describes the temperature-dependent region of the T_1^{-1} data is 5000–5500 K for the NIST and $YD_{3.0}$ samples at all measurement frequencies. These values are
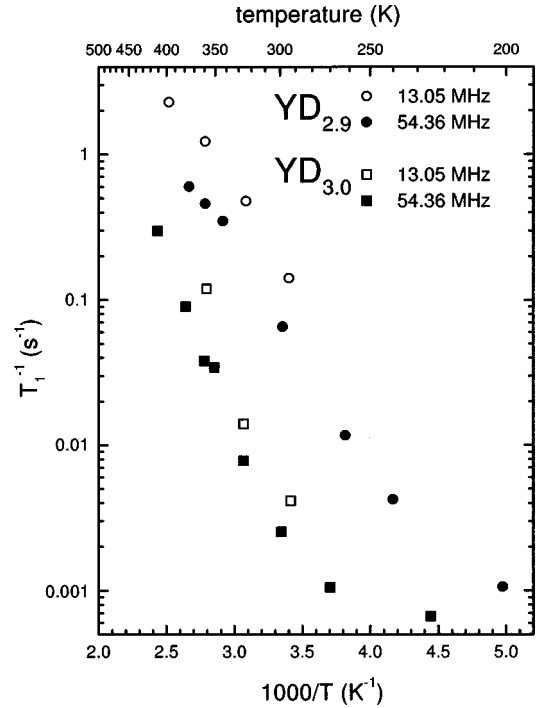
close to the broad approximation of 6000 K found in Eq. (1) describing the rate of diffusion. Second, the rate T_1^{-1} is substantially increased in the $YD_{2.9}$ sample, as is the rate of diffusion. Thus, we propose that deuterium atoms are relaxed by physical diffusion (i.e., not spin diffusion) into the neighborhood of relaxation centers. These centers might be paramagnetic impurities or electrons or holes in deep traps.

In the above model, a D atom makes a diffusive hop every 10 μs at 400 K but it must hop for ≈ 1 s (see Fig. 6) to longitudinally relax. Thus, the atom samples some 10^5 sites to relax, indicating that the relaxation centers are quite dilute, whatever is their nature. While this model offers a natural explanation of the temperature dependence of T_1^{-1} the frequency dependence ($\approx \omega_0^{-0.7}$) is more difficult. Put bluntly, if diffusion is the rate limiting step in the relaxation process, how can there be *any* field dependence? While we cannot explain the exact field dependence, the argument below calculates the field dependence for one kind of relaxation center.

A deuterium atom need not be a nearest neighbor of the relaxation center (an electron spin with a longitudinal relaxation time T_{1e}, we assume) to be relaxed by it. Instead, the D atom need only reside within some critical radius R_0, defining the relaxation sphere. Here we treat the R^{-6} dependence of the direct nuclear relaxation rate from the electron spin to be ''all or nothing''—outside the sphere no direct relaxation occurs, while instantaneous relaxation awaits any deuterium passing into the relaxation sphere. This approximation is coarse but substantially simplifies the analysis. The direct nuclear relaxation rate r will vary as $r \propto R^{-6}T_{1e}$ (i.e., second moment times a correlation time) in the limit that $\omega_0 T_{1e} \ll 1$ (here ω_0 is the nuclear spin angular precession frequency). In the 200–400-K temperature range, electron

T_{1e} values are generally quite short, satisfying this criterion. For a Kramers ion such as Gd^{3+}, T_{1e} can be field dependent because of the need to break time-reversal symmetry so that modulation of ligand fields can induce relaxation transitions. Thus, phonon-driven Raman-process relaxation can have[31] a H^2 (or equivalently ω_0^2) dependence: $T_{1e}^{-1} \propto \omega_0^2$. Thus, nuclear spins are directly relaxed at rate r,

$$r \propto \frac{1}{R^6} \frac{1}{\omega_0^2}. \tag{5}$$

In the all-or-nothing treatment, the radius R_0 of the relaxation spheres is determined by requiring the direct nuclear relaxation rate r to exceed a certain value. Thus, the radius R_0 will vary at any fixed temperature as $R_0^6 \omega_0^2 = \text{const}$, or $R_0 \propto \omega_0^{-1/3}$. We note that the relaxation sphere's radius comes about in an entirely different way than the field-dependent radius of the barrier to spin diffusion.[23]

The rate of deuterium nuclear spin relaxation T_1^{-1} will then be given by the rate that randomly diffusing trajectories cross into the relaxing zones. To calculate the rate of diffusion (at coefficient D) to relaxation zones of radius R_0, we divide the system into volume regions, choosing R_0 as the natural pixel size. This way, the atom is either in a zone or not. The rate γ with which the diffuser jumps on the coarse lattice is given by

$$R_0^2 \approx D\tau = D\gamma^{-1}, \tag{6}$$

$$\gamma \approx \frac{D}{R_0^2}. \tag{7}$$

The fraction of pixels that are relaxation zones is C_{eff} with $C_{\text{eff}} = NR_0^3$, where N is the number density of dilute relaxation centers. The rate ρ of entering these zones is given by

$$\rho = \gamma C_{\text{eff}}. \tag{8}$$

Thus, the rate ρ is given by

$$\rho \approx \left(\frac{D}{R_0^2}\right)(R_0^3 N). \tag{9}$$

Recalling that $R_0 \propto \omega_0^{-1/3}$ at fixed temperature,

$$\rho \propto DN\omega_0^{-1/3}. \tag{10}$$

The $\omega_0^{-1/3}$ frequency dependence is close but not equal to the dependence of the measured T_1^{-1}. However, the above does show a relaxation mechanism in which *diffusion* is the rate-determining step and in which the relaxation rate depends upon field strength.

IV. CONCLUSIONS

The deuterium NMR spectra are not in accord with the ordered HoD_3-like structure proposed on the basis of neutron-powder-diffraction results. It appears that the tetrahedral sites are disordered/distorted at low temperatures. At approximately 350 K, some motion averages away the disorder, leading to a spectrum of three Pake powder doublets. The approximate 1:1:1 intensity ratio is in accord with space group $P6_3cm$, which has two inequivalent groups of three tetrahedral sites each, and has been demonstrated to fit the neutron-diffraction data. There may also be adjustments that can be made to the HoD_3 structure that would split the tetrahedral sites into two distinct groups.

At still higher temperatures (400 K), the Pake doublet features broaden and a sharp central line develops. This spectral change is the result of diffusion, which allows the D atoms to interchange among the several sites. Both the spectral sharpening and the development of the sharp central line occur at a lower temperature in the sample with the most D-atom vacancies, showing that vacancy diffusion is responsible in both cases.

The longitudinal relaxation appears to be controlled by atomic diffusion of the D atoms to dilute paramagnetic relaxation centers. Support for this comes from the increased T_1^{-1} in the sample with the most vacancies and from the similarity of the activation energies describing T_1^{-1} and diffusion. An unusual $\omega_0^{-0.7}$ frequency dependence of T_1^{-1} is observed and it is suggested to be due to a field-dependent radius of the relaxation zones. The exact nature of the paramagnetic centers is unknown, but it is unlikely that they play any role in the electronic, optical, or structural phenomena of this system because they are so dilute.

[1] J. N. Huiberts, R. Griessen, J. H. Rector, R. J. Wijngaarden, J. P. Dekker, D. G. de Groot, and N. J. Koeman, Nature (London) **380**, 231 (1996).

[2] R. Griessen, J. N. Huiberts, M. Kremers, A. T. M. van Gogh, N. J. Koeman, and J. P. Dekker, J. Alloys Compd. **253-254**, 44 (1997).

[3] J. N. Huiberts, J. H. Rector, R. J. Wijngaarden, S. Jetten, D. de Groot, B. Dam, N. J. Koeman, R. Griessen, B. Hjörvarsson, S. Olafsson, and Y. S. Cho, J. Alloys Compd. **239**, 158 (1996).

[4] J. N. Huiberts, R. Griessen, R. J. Wijngaarden, M. Kremers, and C. Van Haesendonck, Phys. Rev. Lett. **79**, 3724 (1997).

[5] A. C. Switendick, Solid State Commun. **8**, 1463 (1970).

[6] J. P. Dekker, J. van Eck, A. Lodder, and J. N. Huiberts, J. Phys.: Condens. Matter **5**, 4805 (1993).

[7] Y. Wang and M.-Y. Chou, Phys. Rev. B **51**, 7500 (1995).

[8] Y. Wang and M.-Y. Chou, Phys. Rev. Lett. **71**, 1226 (1993).

[9] T. J. Udovic, Q. Huang, and J. J. Rush, J. Phys. Chem. Solids **57**, 423 (1996).

[10] P. J. Kelly, J. P. Dekker, and R. Stumpf, Phys. Rev. Lett. **78**, 1315 (1997).

[11] T. J. Udovic, Q. Huang, and J. J. Rush, Phys. Rev. Lett. **79**, 2920 (1997).

[12] K. K. Ng, F. C. Zhang, V. I. Anisimov, and T. M. Rice, Phys. Rev. Lett. **78**, 1311 (1997).

[13] R. Ahuja, B. Johansson, J. M. Willis, and O. Eriksson, Appl. Phys. Lett. **71**, 3498 (1997).

[14] M. Mansmann and W. E. Wallace, J. Phys. (France) **25**, 454 (1964).

[15] M. Forker, U. Hütten, and M. Lieder, Phys. Rev. B **49**, 8556 (1994).

[16] C. P. Slichter, *Principles of Magnetic Resonance*, 3rd ed. (Springer-Verlag, New York, 1990).

[17] N. L. Adolphi, J. J. Balbach, M. S. Conradi, J. T. Markert, R. M. Cotts, and P. Vajda, Phys. Rev. B **53**, 15 054 (1996).

[18] J. J. Balbach (unpublished).

[19] H. T. Weaver, J. Chem. Phys. **56**, 3193 (1972).

[20] P. Vajda, *Handbook on the Physics and Chemistry of Rare Earths*, edited by K. A. Gschneider, Jr. and L. Eyring (Elsevier North-Holland, New York, 1995), Vol. 20.

[21] T.-T. Phua, B. J. Beaudry, D. T. Peterson, D. R. Torgeson, R. G. Barnes, M. Belhoul, G. A. Styles, and E. F. W. Seymour, Phys. Rev. B **28**, 6227 (1983).

[22] M. M. Hoffmann, Ph.D. thesis, Washington University, 1997.

[23] A. Abragam, *Principles of Nuclear Magnetism* (Oxford University Press, London, 1961).

[24] J. T. Markert and R. M. Cotts, Phys. Rev. B **36**, 6993 (1987).

[25] D. Khatamian and F. D. Manchester, Bull. Alloy Phase Diagrams **9**, 252 (1988).

[26] L. N. Yannopoulos, R. K. Edwards, and P. G. Wahlbeck, J. Phys. Chem. **69**, 2510 (1965).

[27] C. E. Lundin and J. P. Blackledge, J. Electrochem. Soc. **109**, 838 (1962).

[28] T. J. Udovic, Q. Huang, and J. J. Rush (unpublished).

[29] T. J. Udovic, Q. Huang, and J. J. Rush, in *Hydrogen in Semiconductors and Metals*, edited by N. H. Nickel, W. B. Jackson, R. C. Bowman, and R. Leisure, MRS Symposium Proceedings No. 513 (Materials Research Society, Pittsburgh, 1998), p. 197.

[30] H. W. Spiess, Colloid Polym. Sci. **261**, 193 (1983).

[31] A. Abragam and B. Bleaney, *Electron Paramagnetic Resonance of Transition Ions* (Clarendon Press, Oxford, 1970).